SCIENTIFIC REPORTS

OPEN

SUBJECT AREAS:
SUPERCONDUCTIVITY
THEORETICAL PHYSICS
ELECTRONIC MATERIALS AND DEVICES
SUPERCONDUCTING MATERIALS

Received
14 February 2012

Accepted
11 April 2012

Published
25 April 2012

Correspondence and requests for materials should be addressed to H.D. (dingh@iphy.ac.cn)

Local antiferromagnetic exchange and collaborative Fermi surface as key ingredients of high temperature superconductors

Jiangping Hu[1,2] & Hong Ding[1]

[1]Beijing National Laboratory for Condensed Matter Physics, and Institute of Physics, Chinese Academy of Sciences, Beijing 100190, China, [2]Department of Physics, Purdue University, West Lafayette, Indiana 47907, USA.

Cuprates, ferropnictides and ferrochalcogenides are three classes of unconventional high temperature superconductors, who share similar phase diagrams in which superconductivity develops after a magnetic order is suppressed, suggesting a strong interplay between superconductivity and magnetism, although the exact picture of this interplay remains elusive. Here we show that there is a direct bridge connecting antiferromagnetic exchange interactions determined in the parent compounds of these materials to the superconducting gap functions observed in the corresponding superconducting materials: in all high temperature superconductors, the Fermi surface topology matches the form factor of the pairing symmetry favored by local magnetic exchange interactions. We suggest that this match offers a principle guide to search for new high temperature superconductors.

In a conventional superconductor, superconductivity emerges from a normal metallic state below a critical transition temperature T_c, when pairs of electrons with opposite momenta near the Fermi surface (FS) are bound together to form a Cooper pair by an attractive force generated through absorption and emission of phonons. The pairing strength can be determined by measuring an energy gap, Δ, which equals $1.76k_BT_c$ in a standard BCS superconductor[1]. Within this traditional picture of superconductivity, magnetism is considered to be an enemy of superconductivity because it breaks Cooper pairs. Furthermore, if the phases of Cooper pairs change signs in the reciprocal space, even non-magnetic impurities are harmful to superconductivity[2]. In contrast, the three known classes of high-T_c superconductors (HTSCs) apparently violate many of these conventional wisdoms[3,4]. First, the superconductivity in these HTSCs develops from a 'bad metal' state whose resistivity is several orders of magnitude higher than those of BCS superconductors. Second, strong magnetism is involved in the 'bad metal' parent state and the superconductivity occurs when long-range magnetic order is suppressed. Third, the ratio of Δ/k_BT_c is much larger than 1.76[5–11]. Finally, the superconducting states are rather robust against impurities[4,12], contrary to conventional superconductors.

The studies of high-T_c cuprates have led to many different proposals of superconducting mechanisms[3,13–15]. In general, we can divide these proposals into three categories: (i) superconductivity without involving magnetism; (2) superconductivity mediated by spin fluctuations; (iii) superconductivity emerging from doped antiferromagnetic (AF) Mott insulators. The first category ignores the connection between magnetism and superconductivity. The difference between the second and the third categories is that the former suggests superconductivity mainly depends on the properties near Fermi surface in reciprocal space and Cooper pairs are formed by the retarded attractive force generated through emitting and absorbing "gluon", in this case, magnons, while the latter emphasizes local interactions in real space and short-range magnetic exchange interactions are responsible for superconducting pairing. The discoveries of iron-based superconductors demonstrate again strong interplay between magnetism and superconductivity, as their phase diagrams are very similar to those of cuprates. However, while iron-based superconductors can reach T_c comparable to single layer cuprates, they are much more itinerant than cuprates[4]. Moreover, between two classes of iron-based superconductors, ferropnictides are also more itinerant than ferrochalcogenides even through T_c in both materials are also similar. Therefore, a unified mechanism of high T_c must reconcile the variation of the degree of itinerancy, a property in the reciprocal space, with magnetic interactions in real space. Here we show that, disregarding many microscopic electronic

differences among the three classes of HTSCs, there exists a basic paradigm to unifiedly understand both cuprates and iron-based superconductors, including ferropnictides and ferrochalcogenides: the key ingredients in the determination of high T_c and pairing symmetries are local AF exchange interactions in real space and Fermi surface topology in reciprocal space that matches to the pairing form factor provided by the AF interactions. Such a paradigm will help to predict new high-T_c superconductors and provide a guide to modify the properties of a material to increase T_c.

Results

Effective magnetic exchange interactions. First, we examine the magnetic exchange interactions of parent compounds of HTSCs. In all three classes of HTSCs, the transition metal atoms form a tetragonal square lattice. Their parent compounds exhibit distinct magnetically ordered states[16–19], as shown in Fig. 1.

In cuprates, the magnetic order is a checkerboard AF state with an ordered wavevector (π,π) as shown in Fig. 1a. This state can be naturally derived from a Heisenberg model where only the nearest neighbor (NN) AF interaction J_1 is important and longer range magnetic exchange interactions can be ignored. Microscopically, J_1 is generated by the superexchange mechanism mediated through oxygen atoms located in the middle of two NN copper atoms.

In ferropnictides, the magnetic order is a collinear AF (CAF) state with an ordered wavevector $(\pi, 0)$[16] as shown in Fig. 1b. This magnetic state can be obtained in a $J_1 - J_2$ Heisenberg model with $J_1 < 2J_2$[20–24], where J_2 is the 2_{nd} NN magnetic exchange interaction. The measurement of spin wave excitations in the parent compounds of ferropnictides indicates that both J_1 and J_2 are AF[25].

In the 11-ferrochalcogenide, FeTe, the magnetic order is a bi-collinear AF (BCAF) state with an ordered wavevector $\left(\pm\frac{\pi}{2},\pm\frac{\pi}{2}\right)$[17,18] as shown in Fig. 1c. To obtain this magnetic state, a third NN (3_{rd} NN) AF exchange coupling J_3 is needed[26–28]. In fact, the analysis of spin wave excitations in FeTe shows that a ferromagnetic (FM) J_1 and an AF J_3 must be included while J_2 does not differ significantly from ferropnictides[29]. The magnetic exchange interactions are confirmed again in the 122-ferrochalcogenide, $K_{0.8}Fe_{1.6}Se_2$, which exhibits a block AF state with an ordered wavevector $\left(\frac{3\pi}{5},\frac{\pi}{5}\right)$[19]. Analyzing spin wave excitations in the block-AF state yields similar magnetic exchange interactions as FeTe[30].

Table 1 summarizes important AF exchange interactions in five different HTSCs. It is worth to note that in both statically ordered CAF and BCAF phases of ferropnictides and ferrochalcogenides, the spin wave excitations suggest that J_1 must have different values on links with different spin configurations. This difference can be explained if a NN biquadratic effective spin interaction[24,28] is included. However, since such a term does not play a role in providing superconducting pairing, we will not discuss it further.

Reciprocal form factors of pairing symmetries and determination of high T_c. Second, we examine the possible pairing symmetries and their reciprocal form factors determined from the corresponding magnetic exchange interactions. For an *s*-wave and *d*-wave spin singlet pairing superconductor, only AF exchange interactions play a role in pairing electrons. The explicit pairing forms determined from the AF magnetic models discussed above for five different HTSCs are listed in Table 1 and their detailed derivation is explained in the supplementary information.

Finally, after knowing the form factors of possible pairing symmetries, one can determine the pairing symmetry and the transition temperature. Taking a one-band system with a single AF magnetic exchange interaction as an example[31], T_c is determined by the following self-consistent meanfield equation as

$$2T_c = J_\alpha \sum_k |f_\alpha(k)|^2 g(x(k,T_c)) \qquad (1)$$

where $g(x) = \frac{tanh(x)}{x}$ and $x(k,T_c) = \frac{\epsilon(k)-\mu}{2T_c}$. $\epsilon(k)$ is the band dispersion and $f_\alpha(k)$ is the corresponding pairing form factor determined by the AF exchange interaction J_α. The function $g(x)$ is always positive and has its maximum value on FSs. In order to obtain nonvanishing T_c in Eq.1, the band dispersion $\epsilon(k)$ has to be strongly renormalized so that J_α is comparable to the band width. Iron-based superconductors are multi-band systems. Similar meanfield treatment has been studied in Refs.[32,33]. These studies also show that the pairing symmetry and T_c are mainly determined by the weight of the form factors near FSs.

Here, rather than performing calculation within a theoretical model, we take band structures of HTSCs measured by angle-resolved photoemission spectroscopy (ARPES) and calculate the overlap between the pairing form factors and the FSs, $\sum_k |f(k)|^2 \delta(\epsilon(k)-\mu)$, which is the value of the quantity on the right side of Eq.1 at zero temperature that approximately determines T_c. The quantitative results of the overlap in five typical HTSCs are summarized in Table 1, and the detailed formula to evaluate the overlap is explained in the supplementary information. One can visualize this overlap by plotting FS and gap function in the same reciprocal space, as shown in Fig. 2.

To demonstrate the importance of this overlap in achieving high T_c, we illustrate the details of FS and superconducting gap of the three classes of HTSCs determined by ARPES: (i) In Fig. 3a, we show a typical FS of cuprates (optimally doped $Bi_2Sr_2CaCu_2O_{8+x}$[5]). In this case, it is clear from Table 1 and Fig. 2 that the *d*-wave form, $cosk_x - cosk_y$, has a much larger overlap with the FS than the *s*-wave form. Indeed, ARPES results strongly support this kind of *d*-wave form, as

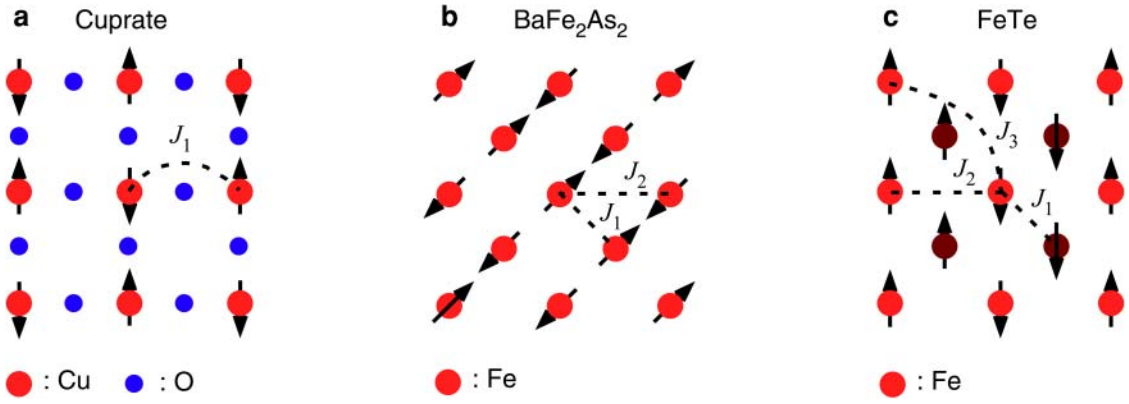

Figure 1 | Magnetically ordered states of HTSCs. (a) checkerboard AF ordering in cuprates. (b) collinear AF ordering in ferropnictides. (c) bicollinear AF ordering in ferrochalcogenides.

Table 1 | Summary of AF exchange interactions, possible reciprocal symmetry forms, and strength of their overlap with FSs (shown as numbers in the table) in five different HTSCs. The numbers with red color indicate the primary superconducting pairings in the corresponding materials. The numbers with parentheses are just for comparison since the corresponding magnetic exchange is FM. The overlap in the electron doped cuprate $Pr_{1-x}Ce_xCuO_4$ is calculated from the band structure measured in ref.[48], showing a smaller value than the one obtained in hole-doped cuprates

AF couplings & gap form	$Bi_2Sr_2CaCu_2O_{8+x}$	$Pr_{1-x}Ce_xCuO_4$	$Ba_{0.6}K_{0.4}Fe_2As_2$	$FeTe_{0.55}Se_{0.45}$	$KFe_{1.7}Se_2$
J_1: *s-wave* $(cosk_x + cosk_y)/2$	0.03	0.01	0.43	(0.29)	(0.01)
J_1: *d-wave* $(cosk_x - cosk_y)/2$	0.61	0.40	0.36	(0.55)	(0.74)
J_2: *s-wave* $cosk_xcosk_y$	–	–	0.62	0.71	0.55
J_2: *d-wave* $sink_xsink_y$	–	–	0.03	0.01	0.05
J_3: *s-wave* $(cos2k_x + cos2k_y)/2$	–	–	–	0.52	0.31
J_3: *d-wave* $(cos2k_x - cos2k_y)/2$	–	–	–	0.07	0.11

shown in Figs. 3d, 3g[5]. (ii) In Fig. 3b, we show the FSs of ferropnictides (optimally hole doped $Ba_{0.6}K_{0.4}Fe_2As_2$[6,8]). There are two hole pockets at Γ, one hole pocket at Z and one electron pocket at M in the unfolded Brillouin zone. In this case, it is also clear from Table 1 and Fig. 2 that the *s*-wave form factor $cosk_xcosk_y$ provided by the 2_{nd} NN AF J_2 has the maximum overlap with the FSs. Consequently, in a doping region where electron and hole pockets are reasonably balanced, an *s*-wave with a symmetry form $cosk_xcosk_y$ should dominate in the superconducting state, which has also been observed by ARPES, as shown in Figs. 3e, 3h[6,8]. However, with a high percentage of hole or electron doping, which destroys the balance between electron and hole pockets, the AF NN J_1 can start to take effect on the pairing symmetry. For example, in the case of heavily hole-doped systems where the FSs are dominated by the hole FS pockets at Γ (Z), the *d*-wave form $cosk_x - cosk_y$ can strongly compete with the *s*-wave form $cosk_xcosk_y$. Indeed, there are strong experimental evidence for gap nodes in the heavily hole-doped superconductor KFe_2As_2 ($T_c \sim 3K$)[34,35]. Such a competition will weaken superconductivity as shown in refs.[32,33]. (iii) In Fig. 3, we plot the FSs of ferrochalcogenides for $FeTe_{0.55}Se_{0.45}$[36], where one hole pocket at Z and one electron pocket at M are observed. In this case, the electron pocket dominates over hole pockets. The *s*-wave symmetry $cosk_xcosk_y$ still has a good overlap with FSs. However, unlike the case of ferropnictides, here the NN interaction J_1 is FM so that there is no competition from the *d*-wave form $cosk_x - cosk_y$. Thus, we still expect a dominant *s*-wave pairing. The presence of a significant 3_{rd} AF J_3 adds interesting effect on the gap function. For an *s*-wave, an AF J_3 provides an additional pairing form, $cos2k_x + cos2k_y$, which takes large values at both hole and

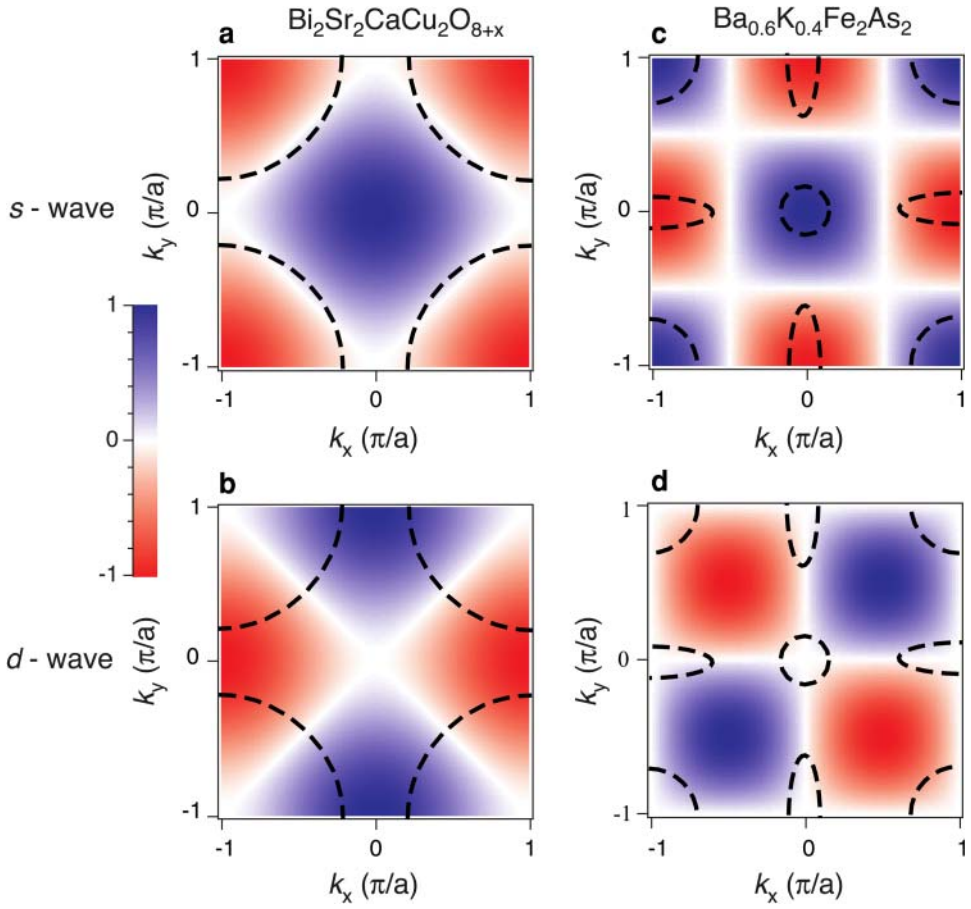

Figure 2 | Visualization of the overlap between FS and gap functions. (a) *s*-wave $cosk_x + cosk_y$ for optimally doped cuprate $Bi_2Sr_2CaCu_2O_{8+x}$. (b) *d*-wave $cosk_x - cosk_y$ for $Bi_2Sr_2CaCu_2O_{8+x}$. (c) *s*-wave $cosk_xcosk_y$ for optimally doped ferropnictide $Ba_{0.6}K_{0.4}Fe_2As_2$. (d) *d*-wave sin_xsink_y for $Ba_{0.6}K_{0.4}Fe_2As_2$. The color bar indicates the values of the superconducting order parameters.

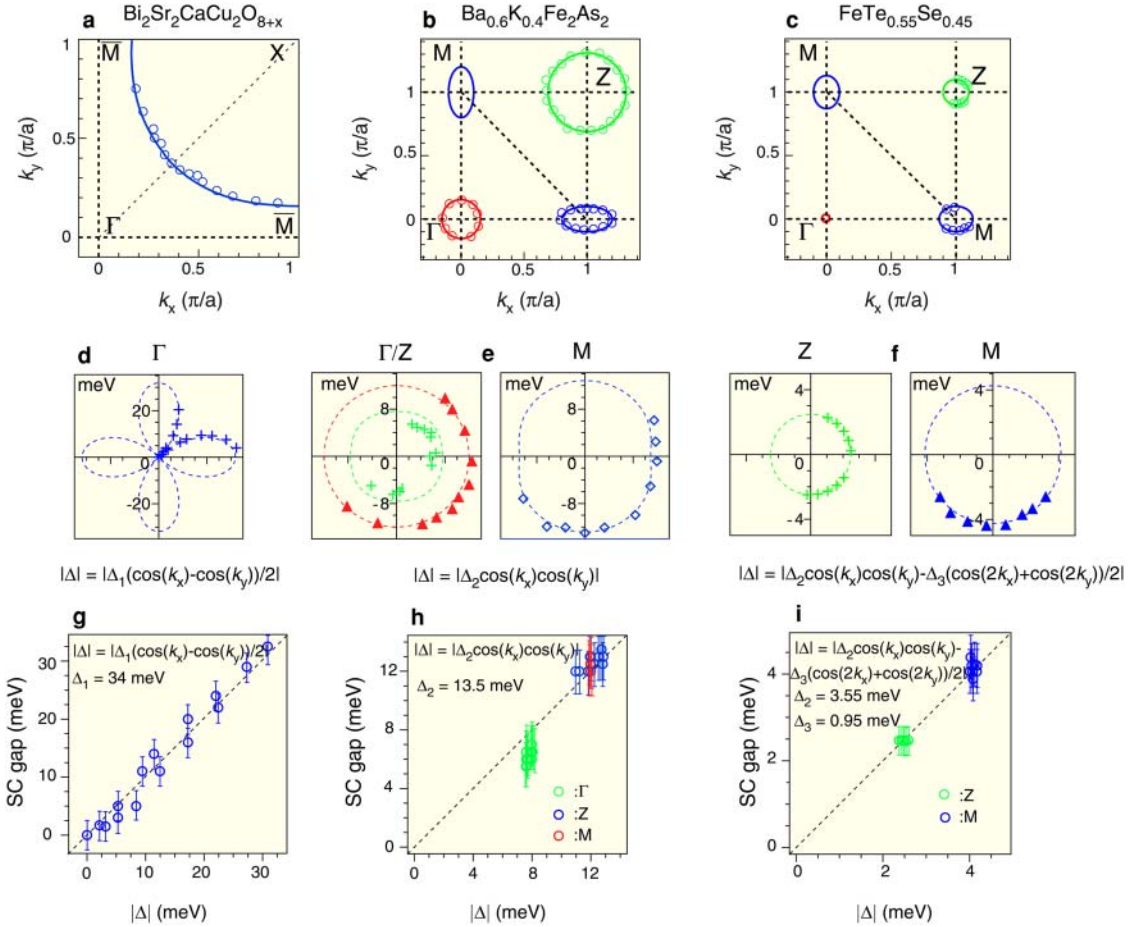

Figure 3 | ARPES results of FS and superconducting gap of HTSCs. FS topologies ((a)–(c)), momentum dependence of the superconducting gap in polar plots ((d)–(f)) (dashed lines are the corresponding gap functions plotted in the panels below), and their fits to reciprocal symmetry forms ((g)–(i)) of three HTSCs: $Bi_2Sr_2CaCu_2O_{8+x}$[5], $Ba_{0.6}K_{0.4}Fe_2As_2$[6,8], and $FeTe_{0.55}Se_{0.45}$[36], respectively.

electron pockets as well. However, unlike $cosk_xcosk_y$ which takes opposite sign between Γ(Z) and M, the form takes the same sign at Γ(Z) and M. Therefore one expects that the pairing form in these materials should be proportional to $cosk_xcosk_y - \delta(cos2k_x + cos2k_y)$ with δ being positive. This pairing form exactly describes what is observed in $FeTe_{0.55}Se_{0.45}$ by ARPES, as shown in Figs. 3f, 3i[36]. The same analysis can also be applied to the recently discovered HTSC $KFe_{1.7}Se_2$, which only has electron pockets at M[9–11,37]. With both J_2 and J_3 being AF, the absence of hole pockets allows the gap function in the electron pockets to take large values to achieve high T_c.

Predictions of possible high temperature superconductors. The paradigm established here allows us to predict possible magnetic interactions and FSs in undiscovered HTSCs. It is clear that the presence of strong local AF interactions is necessary. Assuming that these interactions are known, we can discuss the possible matching FSs which can lead to high-T_c superconductivity in several common lattice structures. In Figs. 4a, 4b, we draw two possible FSs that can lead to high T_c for a tetragonal lattice structure. The FS in Fig. 4a leads to an *s*-wave superconductor for a strong NN AF interaction while the one in Fig. 4b leads to a *d*-wave superconductor for a strong 2_{nd} NN AF interaction. In Figs. 4c, 4d, we draw two FSs that can lead to *s*-wave pairing symmetry in a honeycomb lattice when the NN and 2_{nd} NN AF exchange interactions dominate respectively. The detailed reciprocal pairing forms are given in the supplementary information. The prediction for a triangle lattice with NN AF exchange interactions and *s*-wave pairing symmetry is similar to Fig. 4c with a rotation of 30 degrees of all FS around the center Γ point. We do not address *d*-wave paring symmetry in a honeycomb lattice here because the *d*-wave superconducting state will most likely break the time-reversal symmetry.

Discussion

While the paradigm described here is a phenomenological, or at most, a semi-microscopic understanding of HTSCs, it is already a powerful guide to understand many unconventional properties in these materials.

The paradigm suggests that the effect of electron-electron correlations is very important to high T_c. It can strengthen local AF exchange interactions as well as cause strong renormalization of band structures. However, a strict Mott-insulating state is not a necessity of high T_c. The AF exchange interactions rely more sensibly on the electronic properties of the atoms which mediate superexchange interactions, such as oxygen in cuprates and As or Se(Te) in iron-based superconductors, rather than on-site interaction *U*.

The paradigm also suggests that the sign change of superconducting orders in reciprocal space is not due to the positive Josephson couplings between different FSs. Instead, it is determined together by local AF exchange interactions and FS topology, namely the sign change behavior is a derivative product, rather than an origin to cause high T_c in the first step that has been proposed in many weak coupling theories[38–40]. Of course, Josephson couplings derived in weak coupling theories and superconducting pairing provided by local AF exchange interactions can collaborate with each other to

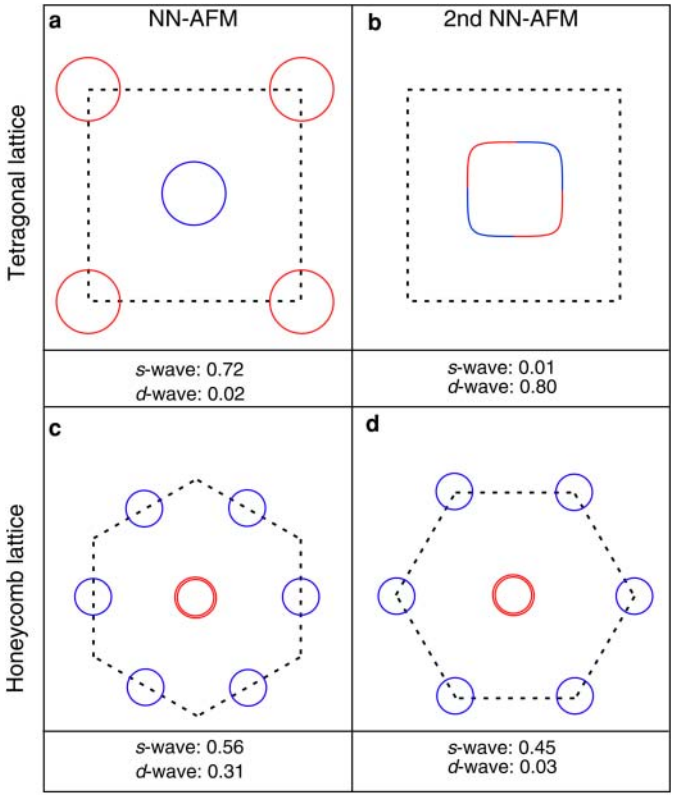

Figure 4 | Predictions of possible collaborative FS topologies and AF exchange interactions that can result in undiscovered high-T_c superconductors. (a) *s*-wave pairing in tetragonal lattice with the NN AF exchange interactions. (b) *d*-wave pairing in tetragonal lattice with the 2_{nd} NN AF exchange interactions. (c) *s*-wave in honeycomb lattice with the NN exchange coupling. (d) *s*-wave in honeycomb lattice with the 2_{nd} NN exchange coupling. The numbers indicate the overlap strength of the corresponding reciprocal symmetry forms on FSs. The red and blue colors indicate the sign change of superconducting order parameters on FSs.

drive higher T_c. Such as in ferropnictides, the collaboration can happen if there are positive Josephson couplings between the hole pockets at Γ(Z) and electron pockets at M. However, in KFe_2Se_2, due to the absence of hole pockets at Γ(Z), the positive Josephson couplings between two electron pockets at M will damage superconductivity if it is *s*-wave pairing. A verification of *s*-wave pairing symmetry in KFe_2Se_2 will be an important support for the paradigm since the positive Josephson coupling between two electron pockets results in a *d*-wave pairing symmetry[41].

The paradigm further provides qualitative explanations of strong pairing, short coherence length and impurity insensitivity in HTSCs. The strong pairing and the short coherence length result from instantaneous and short-range attractive force generated by AF exchange interactions. The superconducting states in all HTSCs are rather robust against nonmagnetic impurities, since the pairing force is determined rather locally and the sign change is due to its form factor derived from local AF exchange. Therefore, if the local AF exchange interactions are not significantly altered by the impurities, the pairing force is stably maintained.

A hidden assumption of the paradigm is that the pairing force can be smoothly derived from the local AF exchange interactions existed in the magnetic parents, which suggests that the leading AF exchange interactions should not be drastically modified in doped materials. This assumption can be tested directly by measuring high-energy spin excitations or other spin properties in doped compounds. In cuprates, recent experiments using resonant inelastic x-ray scattering have reported that many superconductors, encompassing underdoped $YBa_2Cu_4O_8$ and overdoped $YBa_2Cu_3O_7$, exhibits damped spin excitations (paramagnons) with dispersions and spectral weights similar to those of magnons in undoped cuprates[42]. In ferropnictides, similar results have been obtained in the study of $BaFe_{2-x}Ni_xAs_2$ by neutron scattering experiments[43]. Moreover, it has also been shown that the AF J_2 in $Li_{1-x}FeAs$[44], which is already self-doped, is similar to other parent compounds[25,29,30]. In ferrochalcogenides, there is a rather robust incommensurate magnetic excitation in all superconducting $FeTe_{1-x}Se_x$ samples[45–47], which suggests J_3 is rather robust.

In summary, we have demonstrated that the superconducting gap symmetry and amplitude of cuprate, ferropnictide, and ferrochalcogenide HTSCs, as observed by ARPES, can be naturally determined by the local AF exchange interactions of their magnetic parent compounds collaborating with the FS topology in the superconducting offspring compounds. By identifying local AF exchange and collaborative FSs as key ingredients of HTSCs, we are able to predict magnetic configuration, FS topology and pairing symmetry of several undiscovered HTSCs. We believe that this phenomenological description can help to develop a microscopic theory of unconventional high-temperature superconductivity.

1. Bardeen, J., Cooper, L. N. & Schrieffer, J. R. Theory of superconductivity. *Phys. Rev.* **108**, 1175–1204 (1957).
2. Anderson, P. W. Theory of dirty superconductors. *J. Phys. Chem. Solids* **11**, 26 (1959).
3. Norman, M. R. & Pépin, C. The electronic nature of high temperature cuprate superconductors. *Rep. Prog. Phys.* **66**, 1547 (2003).
4. Johnston, D. C. The puzzle of high temperature superconductivity in layered iron pnictides and chalcogenides. *Advances in Physics* **59**, 803 (2010).
5. Ding, H. *et al.* Angle-resolved photoemission spectroscopy study of the superconducting gap anisotropy in $Bi_2Sr_2CaCu_2O_{8+x}$. *Phys. Rev. B* **54**, R9678 (1996).
6. Ding, H. *et al.* Observation of Fermi-surface-dependent nodeless superconducting gaps in $Ba_{0.6}K_{0.4}Fe_2As_2$. *Europhys. Lett.* **83**, 47001 (2008).
7. Zhao, L. *et al.* Multiple nodeless superconducting gaps in $(Ba_{0.6}K_{0.4})Fe_2As_2$ superconductor from angle-resolved photoemission spectroscopy. *Chin. Phys. Lett.* **25,** 4402 (2008).
8. Nakayama, K. *et al.* Superconducting gap symmetry of $Ba_{0.6}K_{0.4}Fe_2As_2$ studies by angle-resolved photoemission spectroscopy. *Europhys. Lett.* **85**, 67002 (2009).
9. Wang, X.-P. *et al.* Strong nodeless pairing on separate electron Fermi surface sheets in $(Tl,K)Fe_{1.78}Se_2$ probed by ARPES. *Europhys. Lett.* **93**, 57001 (2011).
10. Zhang, Y. *et al.* Heavily electron-doped electronic structure and isotropic superconducting gap in $A_xFe_2Se_2$ (A=K,Cs). *Nature Mater.* **10**, 273–277 (2011).
11. Mou, D. *et al.* Distinct Fermi surface topology and nodeless superconducting gap in a $(Tl_{0.58}Rb_{0.42})Fe_{1.72}Se_2$ superconductor. *Phys. Rev. Lett.* **106**, 107001 (2011).
12. Balatsky, A. V., Vekhter, I. & Zhu, J. X. Impurity-induced states in conventional and unconventional superconductors. *Rev. Mod. Phys.* **78**, 373 (2006).
13. Lee, P. A., Nagaosa, N., & Wen, X. G. Doping a Mott insulator: Physics of high-temperature *Rev. Mod. Phys.* **78**, 17 (2006).
14. Anderson, P. W. *et al.* The physics behind high-temperature superconducting cuprates: the "plain vanilla" version Of RVB. *J. Phys. Cond. Mat.* **16**, R755-R769 (2004).
15. Scalapino, D. J. The Cuprate Pairing Mechanism: Pairing of Electrons in Superconducting Cuprates. *Science* **284**, 1282 (1999).
16. de la Cruz, C. *et al.* Magnetic order close to superconductivity in the iron-based layered $LaO_{1-x}F_xFeAs$ systems. *Nature* **453**, 899–902 (2008).
17. Bao, W., *et al.* Tunable $(\delta\pi - \delta\pi)$-type antiferromagnetic order in α-Fe(Te,Se) superconductors. *Phys. Rev. Lett.* **102**, 247001 (2009).
18. Li, S. *et al.* First-order magnetic and structural phase transitions in $Fe_{1+y}Se_xTe_{1-x}$. *Phys. Rev. B* **79**, 054503 (2009).
19. Bao, W. *et al.* A novel large moment antiferromagnetic order in $K_{0.8}Fe_{1.6}Se_2$ superconductor. *Chin. Phys. Lett.* **28**, 086104 (2011).
20. Si, Q. & Abrahams, E. Strong correlations and magnetic frustration in the high Tc iron pnictides. *Phys. Rev. Lett.* **101**, 076401 (2008).
21. Fang, C. *et al.* Theory of electron nematic order in LaOFeAs. *Phys. Rev. B* **77**, 224509 (2008).
22. Xu, C. K., Muller, M. & Sachdev, S. Ising and spin orders in iron-based superconductors. *Phys. Rev. B* **78**, 020501(R) (2008).
23. Yildirim, T. Frustrated magnetic interactions, giant magneto-elastic coupling, and magnetic phonons in iron-pnictides. *Physica C* **469**, 425 (2009).
24. Wysocki, A. L. Belashchenko, K. D. & Antropov, V. P. Consistent model of magnetism in ferropnictides. *Nature Phys.* **7**, 485 (2011).
25. Zhao, J. *et al.* Spin waves and magnetic exchange interactions in $CaFe_2As_2$. *Nature Phys.* **5**, 555–560 (2009).

26. Ma, F. *et al*. Bi-collinear antiferromagnetic order in the tetragonal α-FeTe. *Phys. Rev. Lett.* **102**, 177003 (2009),
27. Fang, C., Bernevig, B. A. & Hu, J. P. Theory of magnetic order in $Fe_{1+y}Te_{1-x}Se_x$. *EuroPhys. Lett.* **86**, 67005 (2009).
28. Hu, J. P. *et al*. A unified minimum effective model of magnetism in iron-based superconductors. Preprint at http://arxiv.org/abs/1106.5169 (2011).
29. Lipscombe, O. J. *et al*. Spin waves in the (π, 0) magnetically ordered iron chalcogenide $Fe_{1.05}Te$. *Phys. Rev. Lett.* **106**, 057004 (2011).
30. Wang, M. *et al*. Spin waves and magnetic exchange interactions in insulating $Rb_{0.89}Fe_{1.58}Se_2$. *Nature Comm.* **2**, 580 (2011).
31. Kotliar, G. & Liu, J. Superexchange mechanism and *d*-wave superconductivity theory of superconductivity. *Phys. Rev. B* **38** 5142 (1988).
32. Seo, K., Seo, K., Bernevig, B. A. & Hu, J. P. Pairing symmetry in a two-orbital exchange coupling model of oxypnictides. *Phys. Rev. Lett.* **101**, 206404 (2008).
33. Fang, C. *et al*. Robustness of *s*-wave pairing in electron overdoped $A_{1-y}Fe_{2-x}Se_2$. *Phys. Rev. X* **1**, 011009 (2011).
34. Dong, J. K. *et al*. Quantum criticality and nodal superconductivity in the FeAs-based superconductor KFe_2As_2. *Phys. Rev. Lett.* **104**, 087005 (2010).
35. Hashimoto, K. *et al*. Evidence for superconducting gap nodes in the zone-centered hole bands of KFe_2As_2 from magnetic penetration-depth measurements. *Phys. Rev. B* **82**, 014526 (2010).
36. Miao, H. *et al*. Isotropic superconducting gaps with enhanced pairing on electron Fermi surfaces in $FeTe_{0.55}Se_{0.45}$. Preprint at http://arxiv.org/abs/1107.0985 (2011).
37. Qian, T. *et al*. Absence of holelike Fermi surface in superconducting $K_{0.8}Fe_{1.7}Se_2$ revealed by angleresolved photoemission spectroscopy. *Phys. Rev. Lett.* **106**, 187001 (2011).
38. Mazin, I. I. *et al*. Unconventional superconductivity with a sign reversal in the order parameter of $LaFeAsO_{1-x}F_x$. *Phys. Rev. Lett.* **101**, 057003 (2008).
39. Kuroki, K. *et al*. Unconventional pairing originating from the disconnected Fermi surfaces of superconducting $LaFeAsO_{1-x}F_x$. *Phys. Rev. Lett.* **101**, 087004 (2008).
40. Wang, F. *et al*. Functional renormalization-group study of the pairing symmetry and pairing mechanism of the FeAs-based high-temperature superconductor. *Phys. Rev. Lett.* **102**, 047005 (2009).
41. Maiti, S. *et al*. Evolution of superconductivity in Fe-based systems with doping. *Phys. Rev. Lett.* **107**, 147002 (2011).
42. Le Tacon, M. *et al*. Intense paramagnon excitations in a large family of high-temperature superconductors. *Nature Phys.* **7**, 725 (2011).
43. Dai, P. C. *private communications.*
44. Wang, M. *et al*. Antiferromagnetic spin excitations in single crystals of nonsuperconducting $Li_{1-x}FeAs$. *Phys. Rev. B* **83**, 220515 (2011).
45. Lumsden, M. D. *et al*. Evolution of spin excitations into the superconducting state in $FeTe_{1-x}Se_x$. *Nature Phys.* **6**, 182 (2010).
46. Argyriou, D. N. *et al*. Incommensurate itinerant antiferromagnetic excitations and spin resonance in the $FeTe_{0.6}Se_{0.4}$ superconductor. *Phys. Rev. B* **81**, 220503(R) (2010).
47. Lee, S.-H. *et al*. Coupling of spin and orbital excitations in the iron-based superconductor $FeSe_{0.5}Te_{0.5}$. *Phys. Rev. B* **81**, 220502(R) (2010).
48. Richard, P. *et al*. Antiferromagnetism-superconductivity competition in electron-doped cuprates triggered by oxygen reduction. *Phys. Rev. Lett.* **99**, 157002 (2007).

Acknowledgement

We thank P. Richard for many valuable suggestions for the manuscript and H. Miao for assistance in constructing figures. We acknowledge B. A. Bernevig, P.-C. Dai, D.-L. Feng, S. Kivelson, D.-H. Lee, H.-H. Wen, X.-G. Wen, Z.-Y. Weng and T. Xiang for valuable discussions. This work is supported by National Basic Research (973) Program of China (grants No. 2010CB92300), National Science Foundation of China (NSFC-11190024) and Chinese Academy of Sciences (grant No. 2010Y1JB6).

Author contributions:

H.D. performed experiments, J.-P.H. did most of theory, J.-P.H. and H.D. wrote the paper.

Additional information

Supplementary Information accompanies this paper at http://www.nature.com/scientificreports

Competing financial interests: The authors declare no competing financial interests.

How to cite this article: Hu, J. & Ding, H. Local antiferromagnetic exchange and collaborative Fermi surface as key ingredients of high temperature superconductors. *Sci. Rep.* 2, 381; DOI:10.1038/srep00381 (2012).